

# **INTERFACE '89**

This paper was published in the proceedings of the  
KTI Microelectronics Seminar, Interface '89, pp. 209-215.  
It is made available as an electronic reprint with permission of KTI Chemicals, Inc.

Copyright 1989.

One print or electronic copy may be made for personal use only. Systematic or multiple reproduction, distribution to multiple locations via electronic or other means, duplication of any material in this paper for a fee or for commercial purposes, or modification of the content of the paper are prohibited.

# OPTIMUM STEPPER PERFORMANCE THROUGH IMAGE MANIPULATION

Chris A. Mack  
Department of Defense  
Fort Meade, Maryland

*Chris Mack received his B.S. degrees in Physics, Chemistry, Electrical Engineering and Chemical Engineering in 1982. He joined the Microelectronics Research Laboratory of the Department of Defense in 1982 and began work in optical lithography research. He has authored papers in the area of optical lithography and has developed the lithography simulation program PROLITH.*

## ABSTRACT

The advent of flexible steppers, allowing variation in the numerical aperture, partial coherence, and possibly other optical parameters, allows new opportunities for optimization. This paper will discuss a method for picking the optimum numerical aperture and partial coherence for a given mask pattern. The intuitive solution, that the highest possible numerical aperture is the best, is true only when the image is in perfect focus. For moderate amounts of defocus, increasing the numerical aperture may actually decrease the quality of the aerial image resulting in degraded stepper performance. Thus, an optimum numerical aperture and partial coherence will be defined for a given amount of defocus. The use of annular sources of illumination will be shown to give some improvement in high resolution performance.

## INTRODUCTION

A trend is emerging in optical step-and-repeat equipment toward greater flexibility and user control. The latest offering from Ultratech Stepper incorporates a variable numerical aperture objective lens (ranging from 0.2 to 0.4) with variable partial coherence of the illumination.<sup>1</sup> Scanning projection printers from Perkin-Elmer have long been able to pick among many possible wave-

length ranges. The new Micrascan I, the first machine to employ the long awaited "step-and-scan" technology, brings the possibility of variable wavelength to stepper technology.<sup>2</sup> The use of excimer lasers as the light source for deep-UV steppers brings with it the potential for generating an arbitrarily shaped illumination source by scanning the laser in the desired shape.<sup>3</sup>

It is the goal of this paper to investigate the potential advantages of using flexible steppers for "image manipulation," that is, varying the aerial image of a given mask pattern by varying the optical parameters of the stepper. Obviously, the purpose of image manipulation will be to improve the lithographic process in some way. Thus, the first step will be to define some metric or metrics of image quality that can be related directly to lithographic quality. Next, the available optical parameters will be varied and the conditions which give the best image (i.e., the maximum value of the image metric) will be found. The three variables that will be used to manipulate the image will be the objective lens numerical aperture (NA), the partial coherence of the illumination ( $\sigma$ ), and the shape of the illumination source.

## AERIAL IMAGE BEHAVIOR

In previous work<sup>4,5</sup> the advantages and disadvantages of various metrics for image quality were discussed. It was shown that the slope of the log of the aerial image (called the log-slope) is directly proportional to the gradient of photoactive compound and the relative gradient of development rate. Through these relationships, the log-slope is the dominant feature of the aerial image which determines exposure latitude. In general, the value of the log-slope at the mask edge is sufficient to

characterize the image. Another metric which is appropriate for spaces and line-space pairs is the ratio of the maximum intensity (usually the center of the space) to the intensity at the mask edge. This ratio is instrumental in determining the sidewall angle of the resist profile. Thus, the two potential metrics are

$$\frac{\partial \ln I}{\partial x} \quad \text{and} \quad \frac{I(\text{center})}{I(\text{edge})} \quad (1)$$

This work will use the log-slope as the image metric. To begin, the behavior of this metric will be investigated as a function of several imaging variables. In any physical system with more than two variables, the key to understanding the behavior of the system lies in choosing an appropriate graphical representation of the data. A good choice of graphs can make complicated behavior easy to visualize. There are two graphs which will prove useful for understanding image behavior: the log-slope versus linewidth curve and the log-slope defocus curve.

The log-slope linewidth curve will show the effect of increasing linewidth on the quality of the aerial image. Intuitively, one would expect that increasing linewidth would improve the image quality, leveling off at some value for very large features. In fact, the behavior is somewhat more complicated. Before showing the results, the curve can be made universal by scaling all dimensions by  $NA/\lambda$  where  $\lambda$  is the wavelength. Thus, the  $x$  position and the linewidth ( $LW$ ) become normalized to

$$\bar{x} = \frac{x NA}{\lambda}$$

$$k = \frac{LW NA}{\lambda} \quad (2)$$

Note that the normalized linewidth  $k$  is just the constant in the Rayleigh resolution equation.

A plot of normalized log-slope versus normalized linewidth is shown in Figure 1 for equal lines and spaces and a partial coherence of 0.5. There are three regions to this curve. Region (a) corresponds to high resolution features and is thus called the high resolution region. As expected, the image quality increases almost linearly with linewidth. In the low resolution region (c), the log-slope levels off as expected to a value corresponding to an isolated edge. In the medium resolution region (b), however, the behavior is less than obvious. Here, the effects of coherence cause the image log-slope to peak at about  $k=0.85$ . To emphasize the role of coherence in this behavior, Figures 2a) and b) show log-slope linewidth curves for coherent and incoherent light, respectively. The dramatic behavior of the coherent light can be derived analytically, and for equal lines and spaces takes the form

$$\frac{\partial \ln I}{\partial \bar{x}} = \frac{4}{k} N \quad (3)$$

where  $N$  is the number of diffraction orders making it through the lens. At  $k=0.5$ , the  $\pm 1$  diffraction orders pass through the lens making  $N=2$ . Thus, the log-slope at this point has a value  $16 \mu\text{m}^{-1}$ . Between  $k=0.5$  and  $k=1.5$  the log-slope goes as  $1/k$ . At  $k=1.5$ , the  $\pm 3$  diffraction orders also make it through the lens. Thus,  $N=4$  and there is a dramatic jump in the value of the log-slope at this point. Likewise, as the linewidth continues to increase, more diffraction orders pass through the lens and there is a discontinuous jump at each value of  $k$  corresponding to a new diffraction order. For incoherent illumination, these discontinuities are effectively averaged out, resulting in a smoother variation.

The effect of defocus on the image can be shown in the log-slope defocus curve.<sup>5</sup> This curve shows the degradation of image quality as the image goes out of focus. Figure 3 shows three log-slope defocus curves corresponding to a given linewidth and three different numerical apertures.

(Note: The curves of Figure 3 as they first appeared in reference<sup>5</sup> were incorrect. An error in the computer program used to generate the curves gave incorrect results for high numerical aperture simulations. This error has since been corrected and the new model has been verified by extensive comparisons with SAMPLE and Doug Goodman's proprietary program IMAGE.)

The important feature of Figure 3 is that the curves cross. When deciding on the best value of NA for this linewidth, one must specify the focal range for which the line is to be printed. If a range of  $\pm 2$  microns or less DOF is required, the high NA lens is definitely preferred. However, higher amounts of defocus show that the lower NA lenses may give better results. Another way to view this effect is to plot log-slope versus NA for different amounts of defocus, as shown in Figure 4. One can see that the optimum value of NA depends on the amount of defocus.

Using the three types of curves described above, it is possible to characterize the effects of variable optical parameters on the image. In general, the optimum set of conditions will depend on the amount of defocus specified. This amount corresponds to the total amount of focus errors built into the process (i.e., the focus budget). Focus budgets of  $\pm 1$  to  $\pm 1.5$  microns are typical.<sup>6</sup>

## IMAGE MANIPULATION

### Numerical Aperture and Partial Coherence

For simplicity, this initial study of image manipulation will involve only equal lines and spaces. The question will be, for a given feature size and focus budget, what are the optimum optical parameters? To be more specific, consider a hypothetical g-line stepper with a variable NA in the range of 0.2 to 0.8, and a partial coherence that can vary between 0.3 and 0.9. Assuming focus budgets of  $\pm 1.0$  and  $\pm 1.5$  microns, what are the optimum NA and  $\sigma$  for a variety of different linewidths? Examining Figure 4, one can see that the

optimum NA for these 0.6 micron line-space pairs is significantly different for the two focus budgets of interest (curves (c) and (d)). Generating multiple curves like Figure 4 for different linewidths and partial coherences, the optimum optical parameters can be determined within the range of our hypothetical stepper. The results are given in Table I.

It is interesting to note that the optimum NA for these focus budgets never exceeds 0.52 down to half-micron feature sizes. There seems little impetus for building higher NA steppers unless the focus budget can be significantly reduced. Also, larger feature sizes require lower NA steppers. For example, a state-of-the-art 0.7 micron production process with a well controlled  $\pm 1$  micron focus budget would perform better on a 0.43 NA stepper than a more costly higher NA machine. Note also that only very high resolution features require the partial coherence to be greater than 0.3.

### Annular Source

The optimum stepper configurations given in Table I assume a standard circular illumination source with a size determined by the partial coherence. Other shapes are possible, however, and may give better results for a given feature. One simple possibility is an annular source. It has long been known that a central obstruction in a circular illumination source can improve resolution.<sup>7</sup> This effect is best illustrated using the log-slope linewidth curve. Figure 5 shows a log-slope linewidth curve (not normalized) for a g-line 0.54 NA stepper with 1 micron of defocus. Curve (a) is the standard circular source with partial coherence of 0.5. Curve (b) shows a thin annular source centered at  $\sigma = 0.5$ . The annular source boosts the log-slope of high resolution features at the expense of lower response for medium resolution features. Changing the position of the annulus (i.e., the center  $\sigma$ ) moves the region of improved log-slope. Thus, for a given feature it is possible to configure an annular source to optimize the image quality for a given focus budget.

Adding the possibility of an annular source to our hypothetical flexible stepper, the process of picking an optimum NA and center  $\sigma$  for the annulus can be carried out for different focus budgets as was done above for the conventional source. The optimum configuration for half-micron lines and spaces is shown in Table II. To see the advantages of the annular source, Figure 6 compares aerial images for the half-micron space under the optimum stepper conditions for conventional and annular sources with 1 micron defocus. Although the improvement with an annular source is not dramatic, it is significant. This improvement is equivalent to adding 0.3 microns to the total DOF of the annular source compared to the conventional source.

## CONCLUSION

The present and future availability of flexible steppers affords a new level of optimization in the lithographic process. The ability to vary the numerical aperture and the size and shape of the illumination source will allow one to optimize the aerial image for a given feature size and focus budget. As Table I indicates, there is no one set of optimum conditions for all features and focus budgets. Since the manufacture of integrated circuits entails the use of many different lithography steps with many different geometries and topographies, a flexible stepper could improve the quality of each lithography step through image manipulation. This paper represents a first attempt at pointing out the potential benefits of image manipulation. Future work will investigate isolated features and other source shapes.

## REFERENCES

1. A. C. Stephanakis and D. I. Rubin, "Advances in 1:1 Optical Lithography," Optical Microlithography VI, Proc., SPIE Vol. 772 (1987) pp. 74-85.
2. J. D. Buckley and C. Karatzas, "Step and Scan: a Systems Overview of a New Lithography Tool," Optical/Laser Microlithography II, Proc., SPIE Vol. 1088 (1989) pp. 424-433.
3. V. Pol, et al., "Excimer Laser-based Lithography: a Deep Ultraviolet Wafer Stepper," Optical Microlithography V, Proc., SPIE Vol. 633 (1986) pp. 6-16.
4. C. A. Mack, "Photoresist Process Optimization," KTI Microelectronics Seminar, Proc., (1987) pp. 153-167.
5. C. A. Mack, "Understanding Focus Effects in Submicron Optical Lithography," Optical/Laser Microlithography, Proc., SPIE Vol. 922 (1988) pp. 135-148, and Optical Engineering, Vol. 27, No. 12 (Dec. 1988) pp. 1093-1100.
6. B. J. Lin, "Paths to Sub-half-micrometer Optical Lithography," Optical/Laser Microlithography, Proc., SPIE Vol. 922 (1988) pp. 256-269.
7. W. J. Smith, Modern Optical Engineering, McGraw-Hill Co. (New York:1966) p. 323.

Linewidth and Defocus	Numerical Aperture (NA)	Coherence Factor ( $\sigma$ )
0.5 $\mu\text{m}$ line/space $\delta = \pm 1.0 \mu\text{m}$ $\delta = \pm 1.5 \mu\text{m}$	0.52 0.41	0.67 0.82
0.6 $\mu\text{m}$ line/space $\delta = \pm 1.0 \mu\text{m}$ $\delta = \pm 1.5 \mu\text{m}$	0.48 0.42	0.30 0.68
0.7 $\mu\text{m}$ line/space $\delta = \pm 1.0 \mu\text{m}$ $\delta = \pm 1.5 \mu\text{m}$	0.43 0.39	0.30 0.30
0.8 $\mu\text{m}$ line/space $\delta = \pm 1.0 \mu\text{m}$ $\delta = \pm 1.5 \mu\text{m}$	0.39 0.37	0.30 0.30
0.9 $\mu\text{m}$ line/space $\delta = \pm 1.0 \mu\text{m}$ $\delta = \pm 1.5 \mu\text{m}$	0.35 0.34	0.30 0.30
1.0 $\mu\text{m}$ line/space $\delta = \pm 1.0 \mu\text{m}$ $\delta = \pm 1.5 \mu\text{m}$	0.31 0.31	0.30 0.30

Table I: Optimum numerical apertures and coherence factors for a g-line stepper with a conventional source at the given focus budgets.

Linewidth and Defocus	Numerical Aperture (NA)	Center Coherence Factor ( $\sigma$ )
0.5 $\mu\text{m}$ line/space $\delta = \pm 1.0 \mu\text{m}$ $\delta = \pm 1.5 \mu\text{m}$	0.56 0.45	0.48 0.60

Table II: Optimum numerical aperture and center coherence factor for a g-line stepper with an annular source at the given focus budgets.

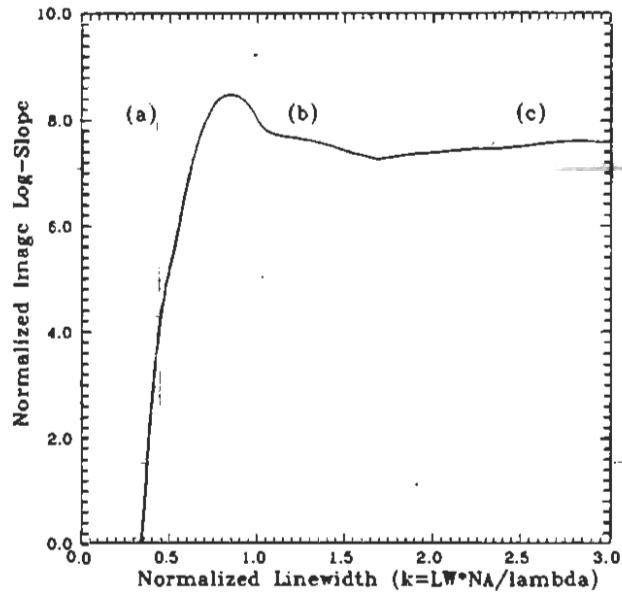


Figure 1: Log-slope linewidth curve ( $\sigma = 0.5$ , equal lines and spaces).

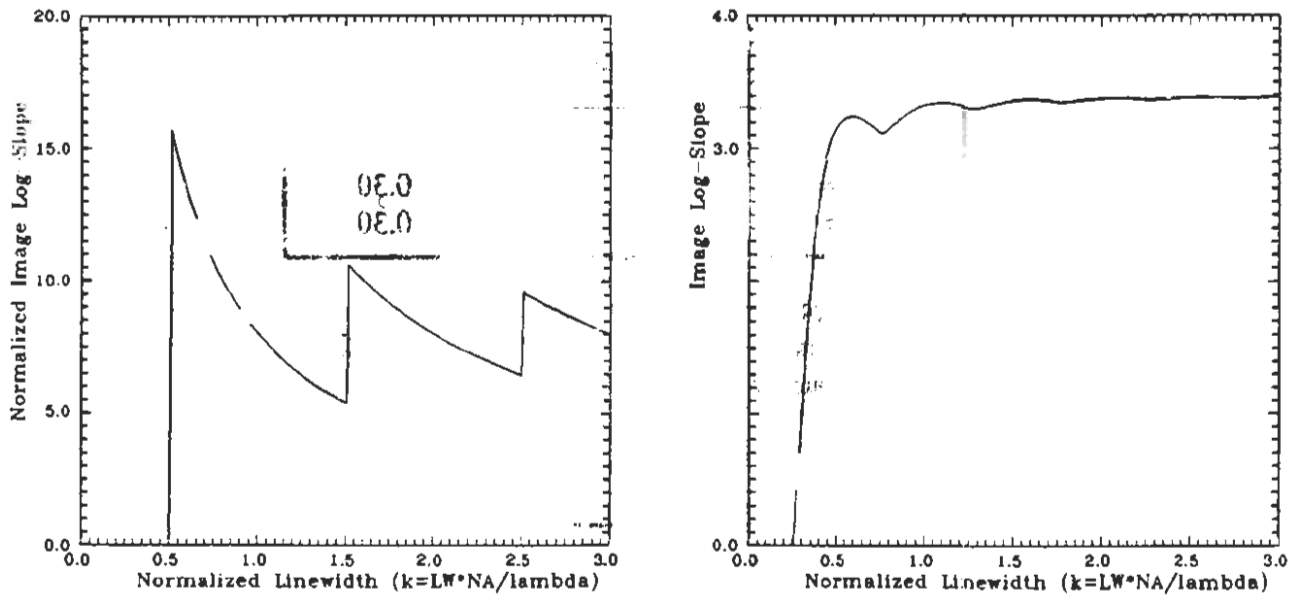


Figure 2: Log-slope linewidth curve for (a) coherent, and (b) incoherent illumination (equal lines and spaces).

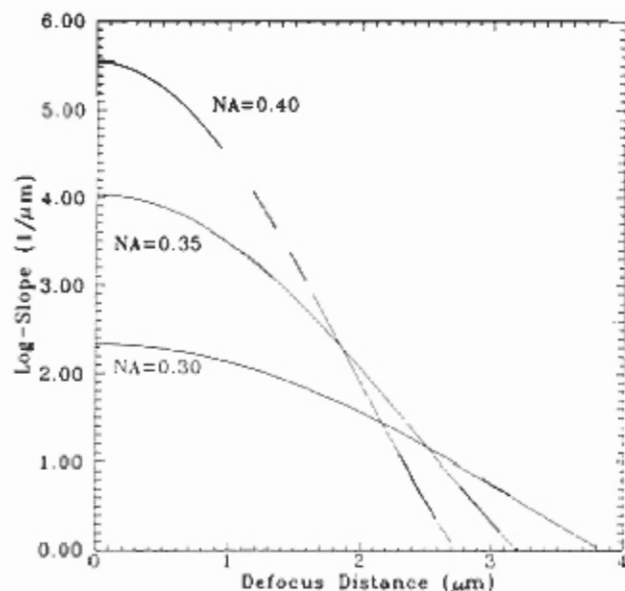


Figure 3: Log-slope defocus curve showing the effect of numerical aperture (0.6 micron lines and spaces, g-line,  $\sigma = 0.5$ ).

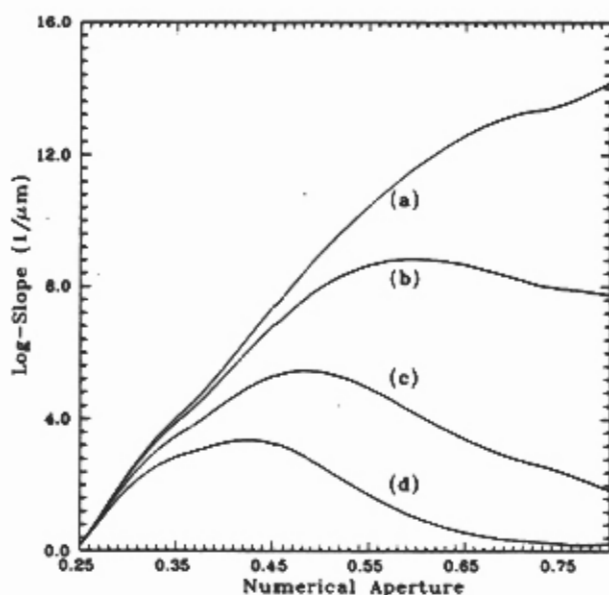


Figure 4: Log-slope versus numerical aperture (0.6 micron lines and spaces, g-line,  $\sigma = 0.5$ ) for (a) in-focus, (b) 0.5 micron defocus, (c) 1.0 micron defocus, and (d) 1.5 microns defocus.

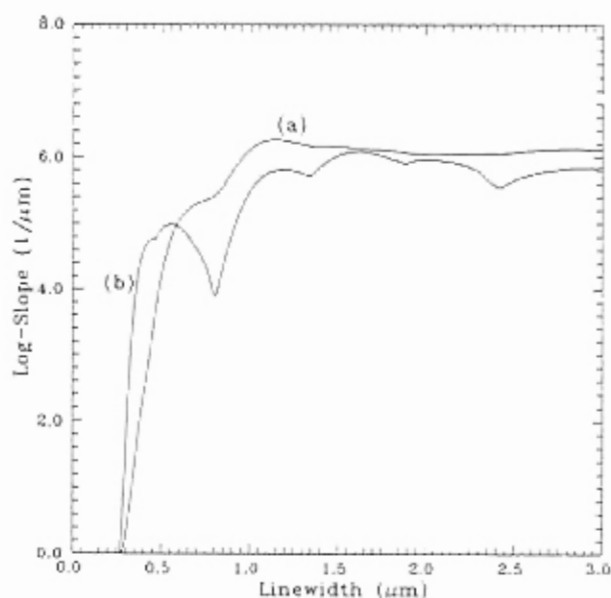


Figure 5: Log-slope linewidth curve (equal lines and spaces, g-line, NA = 0.54, 1.0 micron defocus) for (a) conventional source with  $\sigma = 0.5$ , and (b) thin annular source centered at  $\sigma = 0.5$ .

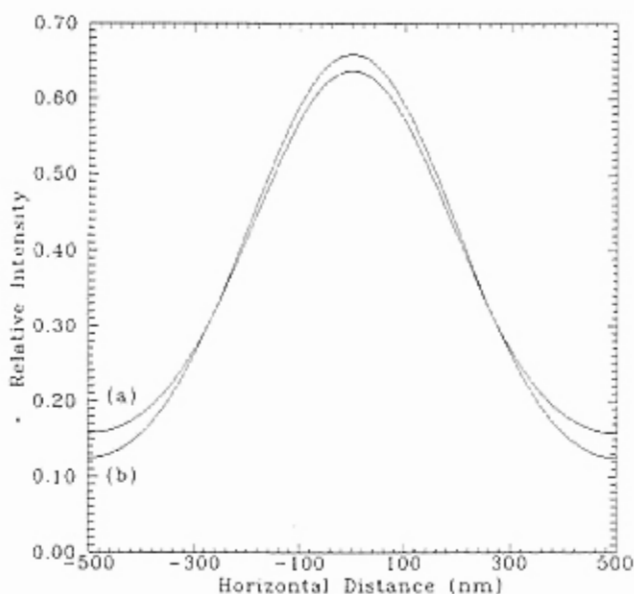


Figure 6: Comparison of the optimum aerial images for 0.5 micron lines and spaces with 1.0 micron defocus for (a) conventional source, and (b) thin annular source, using the parameters in Tables I and II, respectively.





\$29.95

**KTI  
MICROELECTRONICS  
SEMINAR**



---

**PROCEEDINGS**

Sponsored by KTI Chemicals, Inc.  
November 6 - 7, 1989  
San Diego, California